THE ASTROPHYSICAL JOURNAL, 540:489–503, 2000 September 1


# ROTATION OF HORIZONTAL-BRANCH STARS IN GLOBULAR CLUSTERS

ALISON SILLS AND M. H. PINSONNEAULT
Department of Astronomy, Ohio State University, 140 West 18th Avenue, Columbus, OH 43210
*Received 1999 November 2; accepted 2000 January 31*

## ABSTRACT

The rotation of horizontal-branch stars places important constraints on angular momentum evolution in evolved stars and therefore on rotational mixing on the giant branch. Prompted by new observations of rotation rates of horizontal-branch stars, we calculate simple models for the angular momentum evolution of a globular cluster giant star from the base of the giant branch to the star's appearance on the horizontal branch. We include mass loss and infer the accompanied loss of angular momentum for each of four assumptions about the internal angular momentum profile. Mass loss is found to have important implications for angular momentum evolution. These models are compared to observations of horizontal-branch rotation rates in M13. We find that rapid rotation on the horizontal branch can be reconciled with slow solid body main-sequence rotation if giant-branch stars have differential rotation in their convective envelopes and a rapidly rotating core, which is then followed by a redistribution of angular momentum on the horizontal branch. We discuss the physical reasons that these very different properties relative to the solar case may exist in giants. Rapid rotation in the core of the main-sequence precursors of the rapidly rotating horizontal-branch star or an angular momentum source on the giant branch is required for all cases if the rotational velocity of turnoff stars is less than 4 km $s^{-1}$. We suggest that the observed range in rotation rates on the horizontal branch is caused by internal angular momentum redistribution, which occurs on a timescale comparable to the evolution of the stars on the horizontal branch. The apparent lack of rapid horizontal-branch rotators hotter than 12,000 K in M13 could be a consequence of gravitational settling, which inhibits internal angular momentum transport. Alternative explanations and observational tests are discussed.

*Subject heading:* stars: evolution — stars: horizontal-branch — stars: rotation

## 1. INTRODUCTION

There is compelling evidence for extensive mixing in the envelopes of low-mass evolved stars, which is not predicted to occur in classical stellar models. Rotation is frequently invoked, at least implicitly, as the underlying agent that is responsible. There has been extensive work on rotational mixing in both low- and high-mass main-sequence stars (Michaud & Charbonneau 1991; Talon et al. 1997), and phenomenological work on mixing in evolved stars has recently been undertaken by several groups (Charbonnel 1995; Sweigart 1997; Boothroyd & Sackmann 1999). However, detailed physical models of giant-branch mixing have proven to be a significant challenge to theorists.

The largest uncertainty, in our view, has been the lack of constraints on the angular momentum evolution from the main sequence to the first ascent giant branch, the horizontal branch, and beyond. In this paper we examine the implications of measured surface rotation rates of horizontal-branch stars for angular momentum evolution on the giant branch. We will show that the combination of rapid horizontal-branch rotation and slow main-sequence rotation places strong constraints on the angular momentum evolution of giants.

The pioneering work of Sweigart & Mengel (1979) remains the single best physical analysis of rotational mixing in evolved stars. They investigated the link between classical meridional circulation and the CNO anomalies in giants and stressed the initial angular momentum budget and the rotation law in the convection zone. They concluded that meridional circulation was generally consistent with the observational data, provided that the rotation rate on the giant branch was sufficiently high. The necessary rotation rates on the giant branch require a rapidly rotating core on the main sequence, and the convective envelope of a giant-branch star cannot be rotating as a solid body since the required main-sequence rotation rates would be much higher than observed. This study neglected the mixing of elements caused by differential rotation with depth in the star and did not include the effects of mass loss.

Ideally, we would like to study the rotation rates of giant-branch stars directly. These stars show the strongest evidence for nonstandard mixing, and their evolution from main-sequence stars is direct and well understood. By looking at the rotation rates of giants at different luminosities on the giant branch, we should be able to determine their initial angular momentum profile as angular momentum is dredged up by the deepening convection zone. We should also be able to test the predicted correlations between different internal rotation velocities and the observed surface abundances. However, since giant-branch stars are so large, their surface rotation rates are predicted to be very small, much less than 1 km $s^{-1}$. The spectral resolution required to observe such velocities is far beyond what can be achieved today, although gravitational microlensing may make this possible (Gould 1997).

Fortunately, horizontal-branch stars have observable rotation rates, and they provide insight into the interiors of giant stars. Since stars lose mass on the giant branch, the surface of the horizontal-branch star was once inside the giant-branch star. Stars at different effective temperatures on the horizontal branch have lost different amounts of mass and therefore can be used to test the angular momentum distribution within giants. The rotation of stars on the horizontal branch therefore provides an indirect test of the internal rotation of the same stars in previous evolutionary stages.

Observations of rotation rates of horizontal-branch stars are scarce. Rotational velocities for horizontal-branch stars with temperatures between 7000 and 11,000 K have been measured in six globular clusters and the field (Peterson 1983, 1985a, 1985b; Peterson, Tarbell, & Carney 1983; Peterson, Rood, & Crocker 1995; Cohen & McCarthy 1997), and rotation rates for stars up to 20,000 K have been measured only in M13 (Behr et al. 2000). The cooler horizontal-branch stars show a range of rotation rates, both between and within clusters. These stars are rotating at between 10 and 40 km $s^{-1}$, much faster than the rotation rates of a few kilometers per second seen for the Sun and other old main-sequence stars. The usual explanation for this increase in rotation rate between the main sequence and the horizontal branch is that the cores of main-sequence stars retain a substantial fraction of their initial angular momentum and are rotating rapidly. This scenario, which conflicts with helioseismic observations of the slowly rotating solar core, will be tested in this work.

Pinsonneault, Deliyannis, & Demarque (1991) studied the angular momentum evolution of stars as they evolve up the giant branch on to the horizontal branch as a constraint on the amount of internal rotation allowed. They found that differential rotation with depth, rather than solid body rotation, was consistent with the existing observational data. Since that paper, there have been important advances that have prompted us to follow up their work in this paper. The helioseismic observations of the rotational splittings of solar $p$-modes strongly suggest that the Sun is rotating almost as a solid body down to 0.2 $R_\odot$ (Chaplin et al. 1999; Lazrek et al. 1996; Corbard et al. 1998). A stringent test of halo star rotation also comes from very high resolution and signal-to-noise ratio studies of the $^6$Li to $^7$Li abundance ratio in metal-poor halo stars. No evidence for extra line broadening above the 4 km $s^{-1}$ level was found, although line broadening at that level was needed to explain the data (Hobbs, Thorburn, & Rebull 1999). The previous high-resolution spectroscopy studies of main-sequence stars in the halo resulted in observational limits on their rotation rate of 8 km $s^{-1}$ (Carney & Peterson 1981). We also have stronger constraints on the timescale for internal angular momentum transport in main-sequence stars from studies of young open clusters (Sills, Pinsonneault, & Terndrup 2000, and references therein). Finally, we now have observational data for stars on the horizontal branch hotter than 12,000 K in M13, which show a markedly different behavior from the cooler horizontal-branch stars in that cluster—they are all rotating at less than 10 km $s^{-1}$ (Behr et al. 2000). This difference in behavior of horizontal-branch stars of different masses could prove enlightening for questions of horizontal-branch morphology, mass loss on the giant branch, and angular momentum evolution during the horizontal-branch phase.

In this paper, we wish to explore the following question: during the evolution of a star from the main-sequence turnoff to the horizontal branch, how can the star retain a large amount of angular momentum under a relatively limited angular momentum budget and with substantial mass (and hence angular momentum) loss? We begin with a star at the turnoff that is rotating as a solid body, and explore the predicted range of horizontal-branch rotation rates as a function of $T_{\rm eff}$ by considering limiting-case assumptions about the rotation law in the giant star convection zone (solid body or constant specific angular momentum), internal angular momentum transport in giants (conservation of specific angular momentum in the core or all angular momentum is in the convective envelope), and internal angular momentum transport on the horizontal branch (solid body rotation or local conservation of angular momentum between the giant-branch tip and the horizontal branch). In § 2, we outline the method we used to construct our stellar models. We present the results in § 3 and discuss the implications in § 4. A summary of our conclusions is given in § 5.

## 2. METHOD

### 2.1. *The Evolutionary Models*

We used the Yale Rotating Evolution Code (YREC; see Sills et al. (2000)) to calculate a standard nonrotating stellar model from the main sequence up the giant branch to the helium core flash. This model was chosen to have parameters appropriate for stars in M13: $M = 0.8\ M_\odot$, $Z = 0.0006$ ([Fe/H] $= -1.5$), and $Y = 0.23$. The turnoff age of this star is 14.7 Gyr. The mixing length parameter, set by calibrating a solar model, was 1.7. We used OPAL opacities (Iglesias & Rogers 1996) for temperatures greater than $\log T = 4.0$, Alexander & Ferguson (1994) opacities for lower temperatures, the Saha equation of state, and gray Eddington atmospheres. The choice of the equation of state and atmospheres was made necessary by the range of evolutionary stages that we are investigating. The more recent, and more accurate, equations of state (Rogers, Swenson, & Iglesias 1996; Saumon, Chabrier, & Van Horn 1995) and atmospheres (Allard & Hauschildt 1995) unfortunately do not yet extend to the temperatures and densities required for stellar models near the tip of the giant branch. However, since this work is an initial study of rotational evolution in these advanced phases, the qualitative results presented here will not be affected by minor changes in the position of the evolutionary track in the H-R diagram.

### 2.2. *Initial Angular Momentum Budget*

Helioseismology can be used to infer the internal rotation profile of the Sun by observing the rotational splitting of solar $p$-modes. The results imply that the Sun's radiative core is rotating as a solid body down to about $R = 0.2\ R_\odot$, with some disagreement about deeper layers (Chaplin et al. 1999; Lazrek et al. 1996; Corbard et al. 1998). The angular velocity of the solar surface convection zone is dependent on latitude but not on radius (Thompson et al. 1996). Old metal-poor stars do not have similar direct constraints on their internal rotation, but the solar case is certainly a good first approximation. We therefore assume solid body rotation throughout the interior of the main-sequence turnoff progenitor and examine whether it is possible to retain sufficient angular momentum to explain the rapid observed horizontal-branch rotation rates.

Our initial conditions therefore reduce to the total moment of inertia at the main-sequence turnoff and the surface rotation rate. An extrapolation of the angular momentum loss model for Population I stars (Sills et al. 2000) yields $v_{\rm surf} = 1$ km $s^{-1}$ at the turnoff and a total angular momentum of $5 \times 10^{47}$ g $cm^2$ $s^{-1}$, compared with $2 \times 10^{48}$ g $cm^2$ $s^{-1}$ for a star rotating at the current observational limit of 4 km $s^{-1}$. (We note that the latter value is comparable to the angular momentum of a solar model that rotates as a solid body). We will therefore consider an initial

angular momentum of $5 \times 10^{47}$ g cm$^2$ s$^{-1}$ as our base case and $2 \times 10^{48}$ g cm$^2$ s$^{-1}$ as our limiting case, with angular momentum distributed as a function of mass the same as in a solid body rotator.

### 2.3. *Mass and Angular Momentum Loss on the Giant Branch*

In main-sequence stars there is efficient angular momentum loss from a magnetic wind. Because of the low predicted surface rotation rates, the amount of angular momentum loss from a magnetic wind is expected to be small on the giant branch. However, large amounts of mass loss on the first ascent giant branch are required to explain the distribution of horizontal-branch star masses (Rood 1973; Lee, Demarque, & Zinn 1990), and the matter at the surface will carry away at least its own local angular momentum. Mass and angular momentum loss was therefore calculated as follows.

Mass loss on the giant branch was calculated using Reimers's formulation (Reimers 1975):

$$\dot{M} = \alpha \frac{L}{gR} M_\odot \text{ yr}^{-1} , \quad (1)$$

where $L$ is the total luminosity, $g$ is the surface gravity, and $R$ is the radius of the star. The constant $\alpha$ can be varied to allow for different amounts of mass to be lost over the entire giant-branch evolution. The mass loss was assumed to begin at the point of maximum convection zone depth in mass (see § 2.4). The loss of mass was taken into account in the evolution of the star.

We calculated the angular momentum lost from the star as it loses mass, following the method used in Pinsonneault et al. (1991). Rotation is not included in the structural evolution of the star, and rotational mixing is not considered in these models. As mass is lost from the star, the fractional angular momentum loss in a given time step is

$$\Delta J = \tfrac{2}{3} \Delta M R^2 \omega , \quad (2)$$

where $\Delta M$ is the total mass lost during the time step, $R$ is the stellar radius, and $\omega$ is the rotation rate at the surface of the star. Models with different mass-loss rates will therefore experience different amounts of angular momentum loss.

The Reimers's mass-loss constant $\alpha$ was varied so that different amounts of mass, up to almost all of the mass outside the helium burning core, were lost from the initially 0.8 $M_\odot$ model. For each of the resulting combinations of core mass (taken from the model at the tip of the giant branch) and envelope mass, we calculated zero age horizontal-branch evolutionary models and determined the star's temperature, radius, total moment of inertia, and moment of inertia of the convection zone on the horizontal branch. The structural properties of each horizontal-branch model are given in Table 1.

The total amount of angular momentum that survives in the convective envelope and radiative core depends not only upon the amount of mass and angular momentum loss but also on the efficiency of internal angular momentum transport from the contracting radiative core into the expanding convective envelope and the angular momentum distribution within the convective envelope. We outline below the limiting cases we have chosen to investigate the different possibilities.

### 2.4. *Internal Redistribution of Angular Momentum from the Turnoff to the Giant-Branch Tip*

The radiative core on the giant branch is a potential reservoir of angular momentum that could be redistributed to the surface layers after the helium flash. There is a significant fraction of the initial mass (0.313 $M_\odot$) that is never incorporated in the outer convective envelope. This inner core contains 16.9% of the moment of inertia, and therefore angular momentum, of the main-sequence turnoff precursor assuming solid body rotation. Another 0.156 $M_\odot$ from the convective envelope falls into the radiative interior between the point of maximum depth in mass and the helium flash; the angular momentum content of this component depends on the angular momentum distribution in convective regions.

We consider two limiting cases for the angular momentum content of the radiative core on the giant branch:

1. *Angular momentum present in the core at the point of maximum convection zone depth or deposited in the radiative core until the tip of the giant branch.*—This assumption preserves the maximum amount of core angular momentum unless angular momentum is pumped into the rapidly rotating core from the slowly rotating envelope. In this first case we assume that the core conserves its total initial angular momentum. This is not necessarily in contradiction with the small degree of internal solar differential rotation inferred from helioseismology given the much shorter timescale for upper giant-branch evolution (18 Myr from the point of maximum convection zone depth to the tip of the red giant branch [RGB], for example) compared with the age of the Sun (4.57 Gyr). We also note that studies of angular momentum evolution in young open cluster stars also require a timescale for internal angular momentum transport between 20 and 100 Myr (Keppens, MacGregor, & Charbonneau 1995; Allain 1998; Sills et al. 2000, and references therein ).

TABLE 1

STRUCTURE OF THE HORIZONTAL-BRANCH STARS

| $\alpha$ | $M_{HB}$ ($M_\odot$) | $R_{HB}$ (cm) | $T_{eff}$ (K) | $I_{tot}$ (g cm$^2$) | $M_{core}$ ($M_\odot$) | $I_{avail}$ (g cm$^2$) |
|---|---|---|---|---|---|---|
| $8.75 \times 10^{-6}$..... | 0.498 | $1.02 \times 10^{10}$ | 31477 | $4.06 \times 10^{51}$ | 0.493 | $2.39 \times 10^{50}$ |
| $8.0 \times 10^{-6}$ ..... | 0.522 | $2.45 \times 10^{10}$ | 20905 | $5.64 \times 10^{51}$ | 0.495 | $1.75 \times 10^{51}$ |
| $7.5 \times 10^{-6}$ ..... | 0.543 | $3.65 \times 10^{10}$ | 17459 | $8.28 \times 10^{51}$ | 0.495 | $4.32 \times 10^{51}$ |
| $6.0 \times 10^{-6}$ ..... | 0.602 | $1.05 \times 10^{11}$ | 11120 | $3.54 \times 10^{52}$ | 0.495 | $3.12 \times 10^{52}$ |
| $5.0 \times 10^{-6}$ ..... | 0.640 | $2.10 \times 10^{11}$ | 8199 | $1.08 \times 10^{53}$ | 0.495 | $1.04 \times 10^{53}$ |
| $4.0 \times 10^{-6}$ ..... | 0.675 | $3.81 \times 10^{11}$ | 6259 | $3.04 \times 10^{53}$ | 0.495 | $2.99 \times 10^{53}$ |
| $2.0 \times 10^{-6}$ ..... | 0.740 | $5.10 \times 10^{11}$ | 5582 | $1.76 \times 10^{54}$ | 0.495 | $1.75 \times 10^{54}$ |

2. *Solid body rotation at all times in the radiative core with* $\omega = \omega_{CZbase}$.—The second assumption is the limit of instantaneous angular momentum transport within the radiative core; this would correspond to solid body rotation in the radiative core of the interior with an angular velocity equal to that of the base of the surface convection zone. Given the small fraction of the total moment of inertia in the radiative core of a giant-branch star (less than 1% at the giant-branch tip), this is effectively equivalent to depositing all of the angular momentum in the convective envelope.

### 2.5. *Rotation Law in Convective Regions*

The principal observational constraint on the angular momentum distribution in convective regions is from helioseismology: the angular velocity is independent of radius in the solar convection zone. However, rotation is much slower on the giant branch, which implies that this may not hold across the large number of pressure scale heights in a giant-branch convective envelope. We therefore consider two limiting cases.

1. *Solid body rotation at all times in convective regions.*—The assumption of solid body rotation at all times in convective regions concentrates high specific angular momentum material in the outer layers of the convection zone. When mass is lost from the star, a higher fraction of the angular momentum of the star goes with it than would be the case if the deeper layers had a larger fraction of the angular momentum. This assumption implies very slow rotation at the base of the convection zone for reasonable initial rotation rates. It is therefore very difficult to drive local mixing in the radiative interior (Sweigart & Mengel 1979).

2. *Constant specific angular momentum at all times in convective regions.*—The assumption of constant specific angular momentum concentrates the envelope angular momentum in the deeper layers of the envelope, with the bulk of the mass. This minimizes the fraction of the envelope angular momentum carried away by mass loss.

### 2.6. *Internal Redistribution of Angular Momentum on the Horizontal Branch*

As a star undergoes the helium flash, its core expands and its envelope contracts, essentially reversing the structural effects of giant-branch evolution. Therefore, any steep angular velocity profile that has been set up by the giant-branch evolution will be smoothed. It is also possible that hydrodynamic mechanisms, triggered by the helium flash, will redistribute angular momentum throughout the star on very short timescales. Therefore, we consider the following two limiting cases.

1. *Solid body rotation of the entire star on the horizontal branch.*—This case corresponds to the maximum redistribution of the angular momentum from the core throughout the star. The rotation rate at the surface of the horizontal-branch star is given by $\omega = J_{\rm tot}/I_{\rm tot}$. This permits angular momentum preserved in the radiative core of the giant-branch precursor to be redistributed to the outer layers of the horizontal-branch star.

2. *Local conservation of angular momentum between the giant-branch tip and the horizontal branch.*—In this case, no angular momentum is redistributed during the helium flash. The specific angular momentum profile of the giant-branch star is simply carried to the new structure of the star on the horizontal branch. The surface rotation rate is given by the specific angular momentum at the surface of the giant-branch star and the radius of the star on the zero-age horizontal branch. In the limit of a very thin surface convective zone on the horizontal branch, the ratio of the horizontal branch to the giant-branch tip rotation velocities is equal to the radius at the giant-branch tip divided by the horizontal-branch star radius.

3. *Angular momentum redistributed outside the hydrogen-burning shell only.*—We also consider this case, under the assumption that mean molecular weight gradients inhibit angular momentum transport.

### 2.7. *Detailed Description of Individual Cases*

The ultimate goal of these calculations is the rotational velocity on the horizontal branch. First, we need to make an assumption about the total amount of angular momentum available at the turnoff, as discussed above. Second, we calculate the rotation rate on the horizontal branch according to one of two scenarios. If we assume local conservation of angular momentum between the tip of the giant branch and the horizontal branch, then the amount of specific angular momentum on the horizontal branch is equal to the specific angular momentum at the tip of the giant branch and

$$J_M(\mathrm{HB}) = \tfrac{2}{3}\omega_{\rm HB} R_{\rm HB}^2 = J_M(\mathrm{tip}) , \tag{3}$$

so that

$$v_{\rm HB} = \frac{3J_M(\mathrm{tip})}{2R_{\rm HB}} . \tag{4}$$

The other extreme is to assume that the horizontal-branch star rotates as a solid body. In this case, the total angular momentum on the horizontal branch is equal to that at the giant-branch tip and

$$v_{\rm HB} = \frac{J_{\rm tot}(\mathrm{tip})}{I_{\rm tot}(\mathrm{HB})} R_{\rm HB} . \tag{5}$$

Therefore, we need four pieces of information from our models: the total angular momentum of the star at the giant-branch tip, the surface specific angular momentum at the giant-branch tip, the moment of inertia of the star on the horizontal branch, and the radius of the star on the horizontal branch. The moment of inertia and the radius are given by the horizontal-branch model. The total angular momentum and the surface value of the angular momentum per unit mass are derived as outlined below for each of the four giant-branch angular momentum distributions.

Case A is the case in which the entire star always rotates as a solid body. The angular velocity $\omega$ is known at all times from $J_{\rm tot} = \omega I_{\rm tot}$, where $I_{\rm tot}$ is the total moment of inertia of the star. Therefore, following Pinsonneault et al. (1991), the fractional angular momentum loss in a given time step is

$$\frac{\Delta J}{J_{\rm tot}} = \frac{2}{3}\frac{\Delta M R^2}{I_{\rm tot}} , \tag{6}$$

where $\Delta M$ is the total mass lost during the time step, $R$ is the radius, and $I_{\rm tot}$ is the total moment of inertia of the star. The total angular momentum lost over the entire giant-

branch evolution is the sum of the individual $\Delta J$, and the specific angular momentum at the surface is given by $J_M = 2/3\omega R^2$

In case B, we assume that the convection zone rotates as a solid body and that the core retains the angular momentum that it had on the main sequence. The initial angular momentum in the core is given by $J_{\rm core} = \omega({\rm MS}) I_{\rm core}({\rm MS})$, where $I_{\rm core}$ is the moment of inertia of the portion of the star on the main sequence that is contained in the radiative interior where the surface convection zone reaches its maximum depth. The amount of angular momentum in the envelope at any given time is determined by two things: the amount of mass lost from the surface of the star ($\Delta M_1$) and the amount of mass that becomes part of the core as the convection zone recedes ($\Delta M_2$). The total angular momentum of the envelope at any given time step is therefore

$$J_{\rm env} = J_{\rm env,old} - \tfrac{2}{3}\omega_{\rm env} R^2_{\rm surface}\,\Delta M_1 - \tfrac{2}{3}\omega_{\rm env} R^2_{CZ{\rm base}}\,\Delta M_2\ . \tag{7}$$

The amount of angular momentum that moves from the envelope to the core as the convection zone recedes is much less than 1% of the total, so we neglected the term second term in equation (7). Therefore, the amount of angular momentum lost during a given time step is given by equation (6), but with $I_{\rm tot}$ replaced with $I_{\rm env}$ and $J_{\rm tot}$ replaced with $J_{\rm env}$. The total angular momentum of this star at the tip of the giant branch is equal to the amount of angular momentum maintained in the envelope plus the initial angular momentum of the core, and the specific angular momentum at the giant-branch tip is given by $J_M = \frac{2}{3}\omega R^2_{\rm tip}$.

Case C is the case in which the core of the star rotates as a solid body at all times with $\omega = \omega_{CZ{\rm base}}$ and the convection zone has constant specific angular momentum. Therefore, the amount of angular momentum per unit mass changes as the star loses mass and as the convection zone depth changes because of structural changes in the giant. The total angular momentum in the core is given by

$$J_{\rm core} = \frac{3 I_{\rm core}\, J_M({\rm env})}{2 R^2_{CZ{\rm base}}}\ , \tag{8}$$

where $J_M$(env) is the specific angular momentum of the convection zone. Since the moment of inertia of the core is much smaller than the total moment of inertia of the star as a whole (less than $2 \times 10^{-5} I_{\rm tot}$), we assumed that the core contained no angular momentum at all; therefore, the specific angular momentum in the convection zone is given by $J_M = J_{\rm tot}/M_{\rm env}$, where $M_{\rm env}$ is the current mass of the convection zone. As the star loses mass, the amount of total angular momentum at each time step is simply $J_{\rm tot} = J_{\rm tot,old} - J_M({\rm env})\Delta M$. The total angular momentum of the star at the tip of the giant branch is determined by summing the losses at each time step.

The final case, case D, is the simplest in which to calculate the amount of angular momentum left at the tip of the giant branch. In this case, the core of the star (as defined in case B) retains its main-sequence angular momentum and the envelope has constant specific angular momentum. The value of $J_M$ is set at the beginning of the calculation to be equated to $J_{\rm env}/M_{\rm env}$, where both quantities are evaluated at the point of maximum convection zone depth, and is not allowed to change throughout the subsequent evolution. In this case, the total amount of angular momentum lost over the entire giant-branch evolution is $\Delta J_{\rm tot} = J_M\,\Delta M_{\rm tot}$.

## 3. RESULTS

### 3.1. *Angular Momentum Evolution from the Turnoff to the Horizontal Branch*

Figure 1 shows the angular momentum evolution of a star from the main sequence to the horizontal branch, demonstrating the effects of the changing structure on the rotation rate of the star. In each panel, we show the angular velocity profile as a function of radius in the star. We have also marked the positions of the center of the hydrogen-burning shell, the radius at which the hydrogen content is 50% by mass, and the base of the surface convection zone. The star shown here has a mass of 0.8 $M_\odot$, and we assume no mass loss or angular momentum loss along the giant branch and no internal transport of angular momentum. All angular momentum evolution is caused by the changing structure of the star. The first panel shows a star at the main-sequence turnoff, which we have assumed is rotating as a solid body ($\omega$ = constant) with radius. The second panel shows the rotation profile of the star at the position on the giant branch where the convection zone reaches its maximum depth in mass. The profile at the tip of the giant branch is shown in the third panel, and the final panel gives the rotational profile on the zero age horizontal branch. The surface rotational velocities and ages of the star are given in each panel.

As the star evolves along the subgiant branch and up the giant branch to the position of the maximum convection zone depth, the core contracts, the convective envelope deepens, and the surface expands. The angular momentum that is found in the convection zone is redistributed according to the rotation law for convection regions (in this case assumed to be solid body), and the core of the star spins up as it contracts. This trend continues for the rest of the giant-branch evolution, up to the tip of the giant branch. As the core contracts, it continues to spin up, while material at the base of the convection zone falls into the hydrogen-burning shell and the surface continues to expand. At the tip of the giant branch, the surface of the star is rotating 100 times slower than it was on the main sequence. During the helium flash, when the star moves from the tip of the giant branch to its position on the horizontal branch, the giant-branch evolution essentially runs in reverse. The surface of the star contracts and the core of the star expands, flattening the rotational profile and raising the surface rotation rate by a factor of $\sim$10. The horizontal-branch star is not rotating as a solid body, but it is much closer to solid body rotation than to the highly differentially rotating giant-branch stars.

Figure 2 shows the impact of mass loss on the evolution of the moment of inertia of the star along the giant branch. We have plotted total moment of inertia of the star as a function of log ($L/L_\odot$) for evolutionary tracks with different amounts of total mass loss. Low on the giant branch, the star does not lose much mass in each time step, so the stars are not significantly different from each other. Near the tip of the giant branch, however, the amount of mass lost from the star increases, which reduces the size of the giant convection zone, resulting in a smaller star and hence a smaller moment of inertia than predicted from non–mass-losing models. The evolutionary tracks used in this paper represent an improvement over the work done in Pinsonneault et al. (1991), in which mass loss was not included in the evolutionary tracks. Under the assumption that the moment of inertia was not significantly affected by the mass

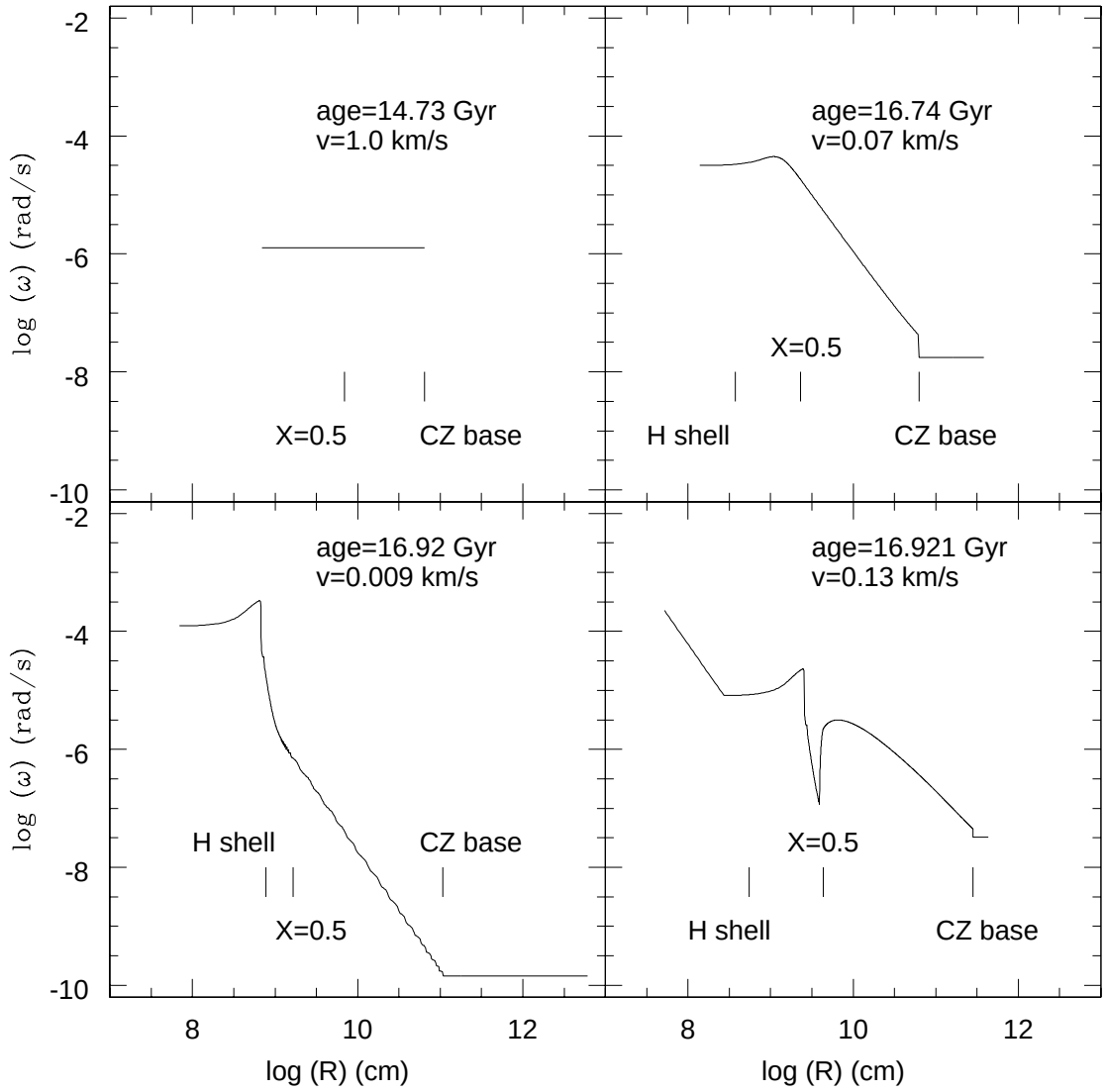


FIG. 1.—Angular velocity evolution of a star as it evolves from the turnoff to the horizontal branch. The 0.8 $M_{\odot}$ star begins as a solid body rotator and then evolves assuming local conservation of angular momentum in radiative regions and solid body rotation in convective regions. There is no mass or angular momentum loss. The four panels show the angular velocity as a function of radius for the turnoff, the position of the maximum convection zone depth in mass, the tip of the giant branch, and the horizontal branch. The tick marks on each panel give the location of (from the center to the surface) the hydrogen-burning shell (not present in the turnoff model), the position at which the hydrogen mass fraction is 50%, and the base of the surface convection zone. The ages and surface rotation velocities are given in each panel.

loss, Pinsonneault et al. (1991) predicted too little angular momentum loss, particularly for the hotter horizontal-branch stars.

### 3.2. *Parameter Variations at Fixed Horizontal-Branch Mass*

We now examine the impact of different assumptions about internal angular momentum transport after the main-sequence turnoff, the rotation profile enforced in convective regions, and internal angular momentum transport during the helium flash and on the horizontal branch.

In Figures 3 and 4 we illustrate the specific angular momentum as a function of mass at different epochs for two different choices of the rotation law in convective regions. In each figure the top panels correspond to the case of solid body rotation at the angular velocity of the base of the surface convection zone, and the bottom set of panels corresponds to the case in which the core conserves its initial angular momentum. We have picked a reference horizontal-branch mass of 0.6 $M_{\odot}$, corresponding to an effective temperature on the horizontal branch of $\sim$10,000 K and total mass loss on the giant branch of 0.2 $M_{\odot}$ . We now discuss results for solid body rotation in convective regions (Fig. 3) and uniform specific angular momentum in convective regions (Fig. 4) in turn.

The assumption of uniform rotation in convective regions implies that the matter at the surface will have relatively high specific angular momentum; as a result, mass loss will effectively drain angular momentum from the envelope (Fig. 3). Furthermore, the base of the surface convection zone will have very low specific angular momentum; this minimizes the angular momentum content of the radiative core even if the core angular momentum is not redistributed to the envelope.

Our reference model at 10,000 K retains from 2% to 18.4% of its turnoff angular momentum, depending on

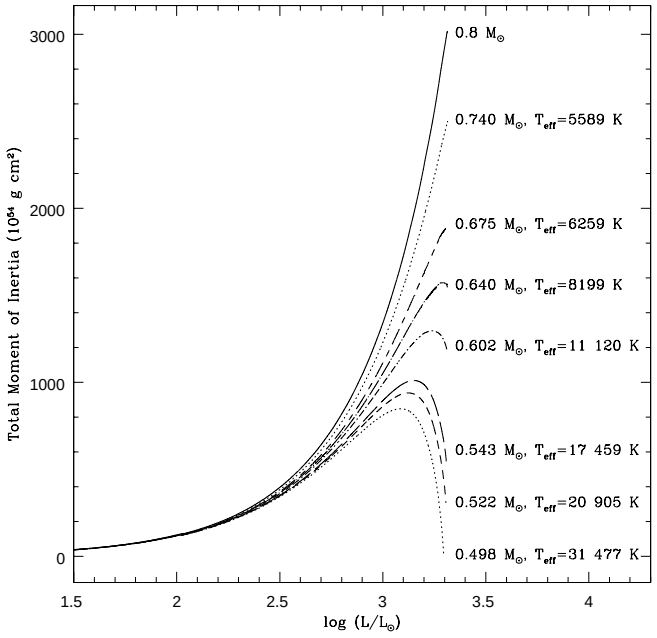


FIG. 2.—Total moment of inertia as a function of luminosity up the giant branch for tracks with different amount of mass loss. The final mass of the star and its effective temperature on the horizontal branch is given on the right side of the graph.

whether solid-body rotation is enforced in the core or whether the angular momentum deposited in the core remains there. Once on the horizontal branch, the surface rotation rate will depend upon whether angular momentum from the core is redistributed to the envelope. For local conservation of angular momentum from the giant-branch tip to the horizontal branch, the predicted surface rotation rates are extremely low, of order 0.01 km $s^{-1}$. If angular momentum is redistributed from the core to the envelope on the horizontal branch the surface rotation rate for our reference model is in the range 0.24 km $s^{-1}$ to 2.23 km $s^{-1}$ depending upon whether or not angular momentum was preserved in the core on the giant branch. The expected surface rotation rates on the horizontal branch for models in this class will be low for all assumptions about internal angular momentum transport on the giant and horizontal branch.

If there is constant specific angular momentum in giant-branch convective envelopes, there are two effects that limit the amount of envelope angular momentum loss. First, the fraction of the envelope angular momentum that is lost is proportional to either the fraction of the mass above the point of maximum convection zone depth (conservation of specific angular momentum in the core) or to the fraction of the convective envelope that is lost (solid body rotation in the radiative core). There will therefore be more angular momentum available on the horizontal branch for this case (Fig. 4). Our reference model retains from 49.8% to 69.4% of its turnoff angular momentum for models with solid body core rotation and constant specific angular momentum in the core, respectively. The inferred surface rotation rates on the horizontal branch range from a low of 0.01 km $s^{-1}$ for local conservation of angular momentum from the giant-branch tip to the horizontal branch to a range of 6.04–8.42 km $s^{-1}$ if there is horizontal-branch angular momentum redistribution.

All of these cases are well below the observed rotation rates of blue horizontal-branch stars, indicating that for solid body main-sequence rotation a main-sequence rotation rate higher than 1 km $s^{-1}$ is needed to explain the data. In the case of solid-body rotation in the convective envelope on the giant branch, the required main-sequence rotation rates are prohibitively high; a similar conclusion was reached in Pinsonneault et al. (1991).

### 3.3. *Trends with Mass on the Horizontal Branch*

Different amounts of giant-branch mass loss will produce horizontal-branch models with different $T_{\rm eff}$: models that lose more mass will also lose more angular momentum. Bluer horizontal-branch models will therefore have systematically less total angular momentum than redder horizontal-branch models. However, the moment of inertia decreases strongly for the bluer horizontal-branch models, and it is therefore not clear a priori that lower surface rotation velocities would be predicted.

The overall structural properties of our horizontal-branch models are summarized in Table 1. All models are shown at the zero-age horizontal branch. There is a strong trend to decreased moment of inertia for the bluer models, which can be easily understood physically. The bulk of the mass is in the core, while the bulk of the moment of inertia is in the envelope. The small change in the total mass at the blue end of the horizontal branch corresponds to a large fractional change in the mass and moment of inertia of the envelope but does not affect the mass of the core.

The fraction of the angular momentum retained under our different cases is illustrated as a function of mass lost on the giant branch in Figure 5; we also present these data in Table 2. The predictions of the different classes of models for the amount of available angular momentum diverge. In the pure solid body model (case A), virtually all of the angular momentum is lost for high giant-branch mass-loss rates. Local conservation of angular momentum in the core and solid body rotation in the envelope (case B) results in a minimum level of angular momentum (retained in the core) even when essentially all of the envelope angular momentum is lost. The two cases with constant specific angular momentum in the convective envelope systematically retain a higher fraction of their turnoff angular momentum; again, the case where a reservoir of angular momentum is retained

TABLE 2

FRACTION OF ANGULAR MOMENTUM RETAINED

| $M_{\rm HB}$ ($M_\odot$) | Case A | Case B | Case C | Case D |
|---|---|---|---|---|
| 0.498..... | $3.0 \times 10^{-8}$ | 0.169 | 0.006 | 0.484 |
| 0.522..... | $6.0 \times 10^{-5}$ | 0.169 | 0.085 | 0.525 |
| 0.543..... | 0.0004 | 0.169 | 0.148 | 0.560 |
| 0.602..... | 0.010 | 0.176 | 0.325 | 0.662 |
| 0.640..... | 0.036 | 0.197 | 0.439 | 0.726 |
| 0.675..... | 0.094 | 0.245 | 0.551 | 0.786 |
| 0.740..... | 0.376 | 0.480 | 0.774 | 0.898 |

NOTES.—Case A: Solid body rotation throughout the star; case B: convection zone rotating as a solid body and core retaining its angular momentum; case C: constant specific angular momentum in the convection zone and no angular momentum in the core; case D: constant specific angular momentum in the convection zone, with the core retaining its angular momentum.

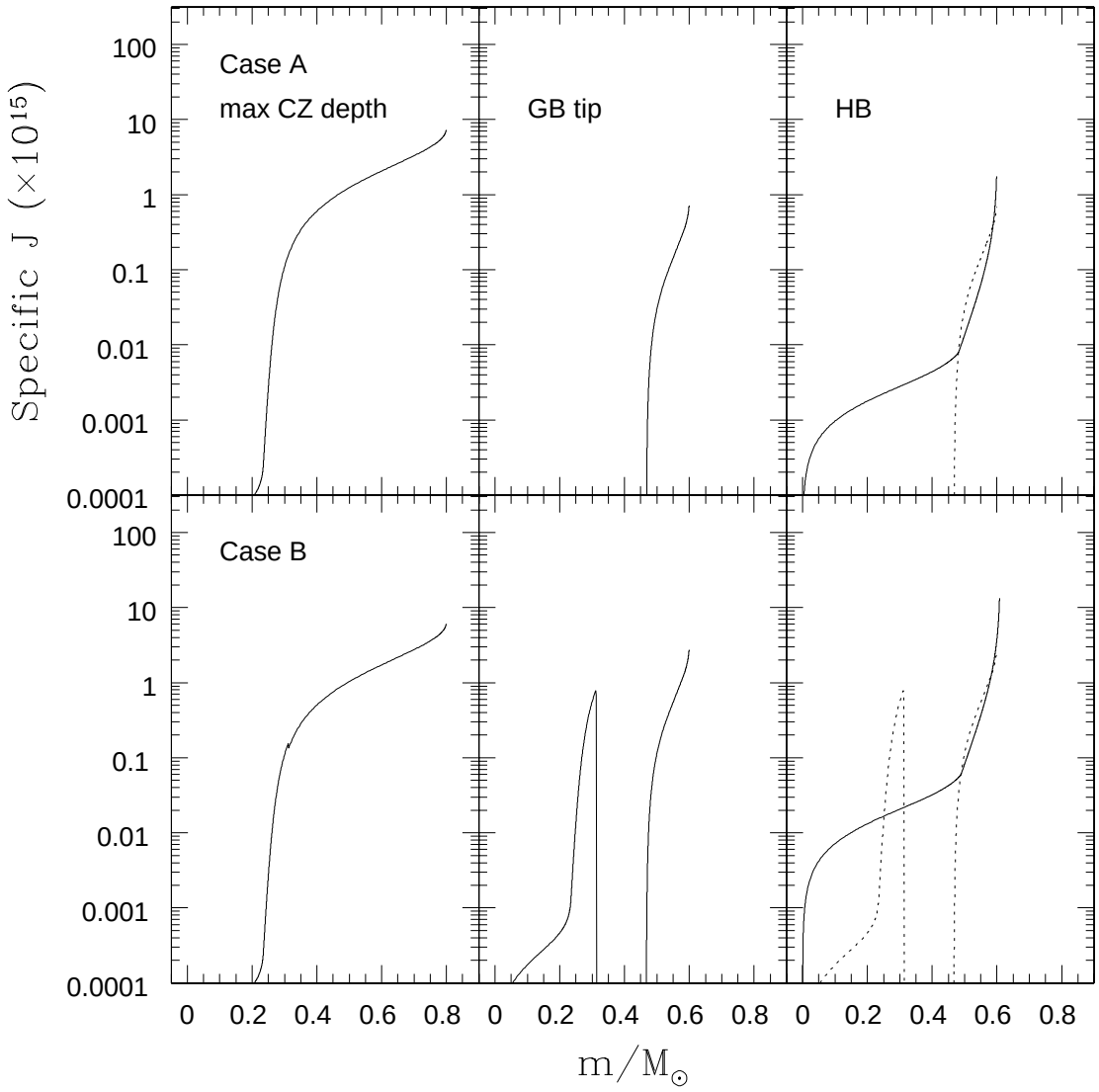


FIG. 3.—Specific angular momentum profiles for a star that begins its life as a 0.8 $M_\odot$ star at the turnoff and then loses mass to become a 0.6 $M_\odot$ star on the horizontal branch. The three panels give the $J/M$ profile for the star at the position of the maximum convection zone depth in mass fraction, the giant-branch tip, and at horizontal-branch profile. The solid line in the third panel assumes a solid body rotation profile throughout the star, and the dotted line shows the profile if there is local conservation of angular momentum between the tip of the giant branch and the horizontal branch. The upper panels show the case in which solid body rotation is enforced throughout the star at all times (case A), and the lower panels show the case in which the core retains its initial angular momentum and the convection zone rotates as a solid body (case B).

TABLE 3

ROTATIONAL VELOCITY

| $M_{HB}$ ($M_\odot$) | ROTATIONAL VELOCITY (km s$^{-1}$), ASSUMING $J_{init} = 5 \times 10^{47}$ g cm$^2$ s$^{-1}$ | | | | | | | |
|---|---|---|---|---|---|---|---|---|
| | Case A-1 | Case B-1 | Case C-1 | Case D-1 | Case A-2 | Case B-2 | Case C-2 | Case D-2 |
| 0.498..... | 0.00 | 2.12 | 0.08 | 6.08 | 0.00 | 0.00 | 0.26 | 0.06 |
| 0.522..... | 0.00 | 3.74 | 1.85 | 11.40 | 0.00 | 0.00 | 0.60 | 0.26 |
| 0.543..... | 0.02 | 3.72 | 3.26 | 12.34 | 0.00 | 0.00 | 0.36 | 0.18 |
| 0.602..... | 0.15 | 2.60 | 4.82 | 9.82 | 0.02 | 0.01 | 0.12 | 0.06 |
| 0.640..... | 0.35 | 1.92 | 4.23 | 7.06 | 0.02 | 0.02 | 0.06 | 0.03 |
| 0.675..... | 0.59 | 1.54 | 3.45 | 4.93 | 0.05 | 0.04 | 0.03 | 0.02 |
| 0.740..... | 0.54 | 0.70 | 1.12 | 1.30 | 0.06 | 0.05 | 0.24 | 0.01 |

NOTES.—Cases A–D are the same as in Figs. 3 and 4 and Table 2. The notation "1" in the case notation indicates models that rotate as solid bodies on the horizontal branch, and "2" indicates models in which local conservation of angular momentum is imposed between the tip of the giant branch and the horizontal branch.

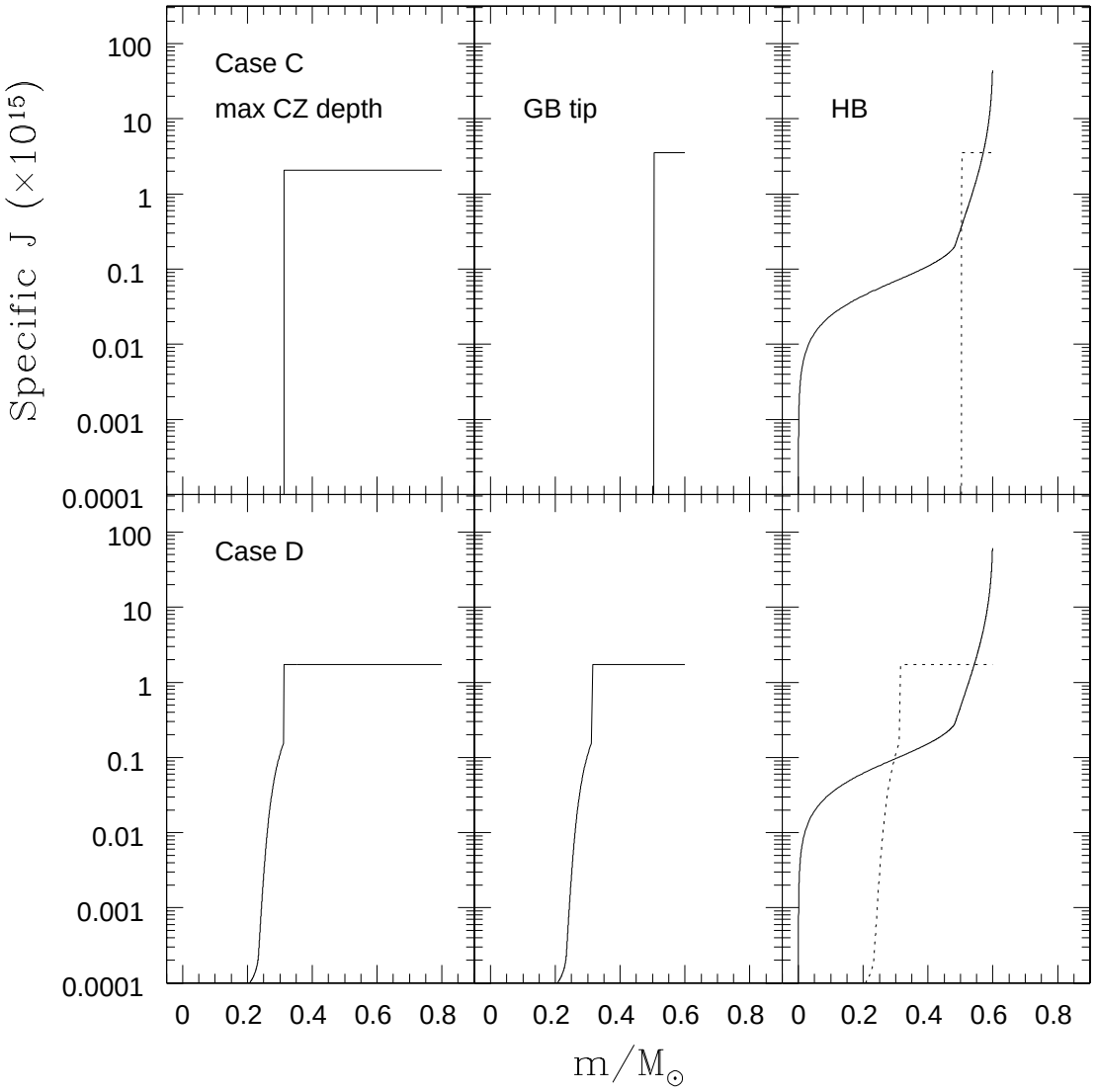


FIG. 4.—As in Fig. 3, but for the two cases in which the convection zone has constant specific angular momentum. The upper panels show the case in which all the angular momentum is constrained to be in the surface convection zone (case C), and the lower panels show the case in which the core retains the angular momentum with which it begins at the turnoff (case D).

in the giant-branch core (case D) leaves more angular momentum than a set of models with solid-body core rotation on the giant branch (case C).

Horizontal-branch surface rotation velocities can be inferred from the angular momentum content and the moment of inertia and radius as a function of $T_{\rm eff}$ (Table 3). All of the cases with local conservation of angular momentum from the giant-branch tip to the horizontal branch have extremely low surface rotation rates (less than 1 km $s^{-1}$). There is a range of higher rotation rates if there is effective angular momentum redistribution during the horizontal-branch phase of evolution. We therefore conclude that a range of surface rotation rates from under 1 km $s^{-1}$ to a ceiling dependent on the prior evolution can be generated on the horizontal branch, and the observed range in rotation rates could reflect evolution on the horizontal branch itself rather than an intrinsic range of initial rotation rates at fixed giant-branch tip mass. We will therefore treat the surface rotation rates for solid body horizontal-branch rotation as an upper envelope; a range of rotation rates up to this level are consistent with the physics of the different cases that we have considered.

We compare the inferred surface rotation rates as a function of $T_{\rm eff}$ with the observational data in Figures 6 and 7. Figure 6 is for a turnoff rotation velocity of 1 km $s^{-1}$, consistent with an extrapolation of the Population I angular momentum loss law to Population II stars; Figure 7 is the same set of cases for a turnoff rotation velocity of 4 km $s^{-1}$, at the level where additional line broadening is observed in high-precision spectroscopic studies of main-sequence halo stars. We note that the upper envelope of the observations in the 4 km $s^{-1}$ case is well matched in the cool horizontal-branch stars ($T_{\rm eff} < 10{,}000$ K), but we predict no decrease in rotational velocities for hotter stars, and no bimodal or sharp cutoff behavior.

## 4. DISCUSSION

Main-sequence metal-poor stars rotate slowly, while some metal-poor horizontal-branch stars are rapid rotators. This combination requires one of the following:

1. Main-sequence stars have a larger angular momentum content than inferred from their slow surface rotation, i.e., they possess rapidly rotating cores;

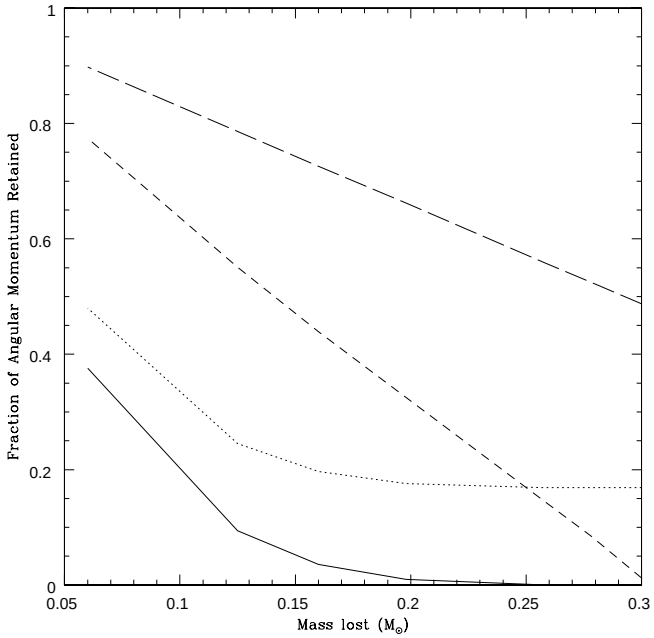


FIG. 5.—Fraction of remaining angular momentum as a function of mass lost for different internal angular momentum profiles. The solid line is the case in which solid body rotation is enforced throughout the star (case A). The dotted line shows the solid body in the convection zone case (case B), the short dashed line has constant specific angular momentum in the convection zone and no angular momentum in the core (case C), and the long dashed line has constant specific angular momentum in the convection zone with a reservoir of angular momentum retained in the core (case D).

2. A significant fraction of a limited angular momentum budget survives extensive giant-branch mass loss; and

3. There is a source of angular momentum for the rapid rotators on the giant branch or during the helium flash.

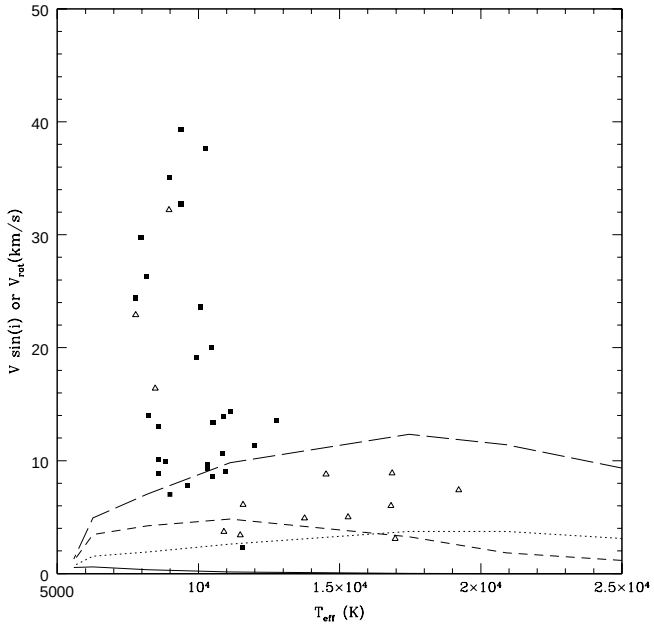


FIG. 6.—Rotational velocity as a function of effective temperature on the horizontal branch for different internal angular momentum profiles. The initial angular momentum at the turnoff was assumed to be $5 \times 10^{47}$ g cm$^2$ s$^{-1}$. The line styles correspond to the same cases as in Fig. 5. The data ($v$ sin $i$) are taken from Peterson et al. (1995; *solid squares*) and Behr et al. (2000; *open triangles*).

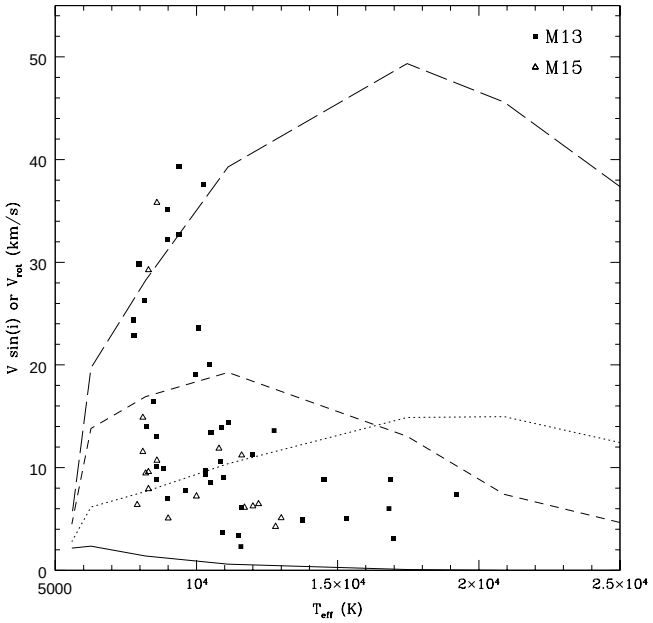


FIG. 7.—Same as Fig. 6, but with an initial angular momentum budget of $2 \times 10^{48}$ g cm$^2$ s$^{-1}$.

We believe that the second explanation is the most likely one and that, by extension, the angular momentum distribution and evolution in evolved stars is very different than that inferred for the Sun. Our results also provide some insight into the role of internal angular momentum transport on the horizontal branch and both the origin of the (real) spread in rotation rates at fixed effective temperature and the surprising temperature dependence of horizontal-branch rotation that has been observed recently. We address these issues individually below.

### 4.1. *Internal Main-Sequence Rotation*

The underlying problem that we are addressing is not new. Pinsonneault et al. (1991) compared the horizontal-branch rotation measurements of Peterson (1983, 1985a) with different theoretical models and concluded that there were two classes of possible solutions: rapid main-sequence core rotation or differential rotation with depth in giant-branch convective envelopes. The strongest other constraints on the internal angular momentum distribution in stars are currently obtained from helioseismology. In 1991, helioseismic inversions were precise enough to rule out strong differential rotation with depth in the solar convection zone but not in the radiative core; therefore, a rapidly rotating core on the main sequence was the favored solution. The advent of more precise helioseismic determinations of the internal solar rotation, however, leads to a fundamental contradiction: either the core rotation of metal-poor main-sequence stars is fundamentally different from the solar case or the convective envelopes of evolved stars are different from the solar convective envelope. A measurement of the surface rotation rates of main-sequence turnoff metal-poor stars will aid in constraining the total amount of angular momentum available during giant-branch evolution.

Our principle result is that a solar-like internal rotation profile on the main sequence can be reconciled with rapid

horizontal-branch rotation and slow main-sequence rotation only if the giant-branch evolution in both the convective envelope and the radiative core is very different during these three evolutionary phases. The one class of models that could reproduce the observed upper envelope of horizontal-branch rotation rates while remaining consistent with the observed limits on main-sequence rotation was the class with constant specific angular momentum in giant-branch convective envelopes, retention of a rapidly rotating core on the giant branch, and subsequent angular momentum redistribution from the core to the envelope on the horizontal branch. Furthermore, even this class of models requires significantly more rapid surface main-sequence rotation ($\sim 4$ km s$^{-1}$) than predicted by an extrapolation of the Population I angular momentum loss law to Population II stars ($\sim 1$ km s$^{-1}$).

There is a possible explanation for metal-poor turnoff stars having higher rotation rates than expected from a straightforward extrapolation of the Population I angular momentum loss law. This would be related to the Population II analogue of the observed Population I break in the rotational properties of high- and low-mass stars (Kraft 1965): low-mass stars experience angular momentum loss and high-mass stars do not. Durney & Latour (1978) used a Rossby scaling argument as follows. There exists a critical rotation rate for a given convective overturn timescale below which a dynamo does not operate. As the convective overturn timescale decreases the critical rotation rate rises; there will therefore be a transition region from low-mass stars that experience angular momentum loss for their entire main-sequence lifetime to higher mass stars that experience spin down only until their surface rotation rate drops below the critical threshold. The convective envelopes of metal-poor turnoff stars are also thin, which suggests that they might experience less angular momentum loss than would be obtained from a prescription without a critical threshold. The convective overturn timescale is a strong function of $T_{\rm eff}$ in the F star regime and also depends on metal abundance. This opens up the further possibility that the available angular momentum budget could depend strongly on metal abundance and age, which could lead to large variations in the degree of rotation in evolved stars and the degree of rotational mixing on the giant branch from modest abundance and age variations.

### 4.2. *Angular Momentum Evolution on the Giant Branch*

If a solar-like internal angular momentum distribution (rotation weakly dependent on depth) is postulated for main-sequence metal-poor stars, strong differential rotation in both the envelopes and cores of giants is required to produce rapid horizontal-branch rotation. This is not necessarily a contradiction given the very different structure and timescale for evolution.

The internal rotation of the Sun as deduced from helioseismology is straightforward. The solar convection zone has differential rotation with latitude but not with depth; there is a shear layer below the convection zone where latitudinal differential rotation vanishes, and below the shear layer the internal solar rotation appears to be nearly independent of both depth and latitude. Because of the short convective overturn timescale in the Sun, a good theoretical case can be made that the properties of the solar convection zone should apply generally when the convective and rotational velocities are of the same order. However, it is far from clear that the same conclusion should be obtained for all convective regions in all stars regardless of the size and rotation rate.

Both the surface and convection zone base rotation velocities are extremely small in giant-branch envelopes because of the small angular momentum reservoir and large moment of inertia. At the point of maximum convection zone depth the rotation velocities at the convection zone base and surface are, respectively, 0.01 and 0.07 km s$^{-1}$ for an initial angular momentum reservoir of $5 \times 10^{47}$ g cm$^2$ s$^{-1}$, solid body rotation in the convective envelope, and no angular momentum loss. At the giant-branch tip these rotation velocities are, respectively, 0.0002 and 0.009 km s$^{-1}$. These velocities are small in comparison with typical convective velocities. By comparison, the solar rotation velocity of 2 km s$^{-1}$ is of the same order or larger than the convective velocity. Therefore, in the Sun, differential rotation with depth would induce a large absolute shear relative to the typical turbulent velocity. In a giant-branch star, however, the convective velocities are so much larger than the rotational velocities that even a large relative gradient in $\omega$ is a small absolute gradient in $\omega$. It is therefore possible that a giant-branch convection zone, even with constant specific angular momentum, would have very little shear and need not rotate as a solid body.

The case of the radiative core is even more complex: the solar data by themselves require effective angular momentum transport by the age of the Sun and by extension also in main-sequence globular cluster stars. However, the solar data do not necessarily require efficient angular momentum transport in radiative regions on much shorter timescales. Several different studies of the angular momentum evolution of low-mass stars have concluded that the timescale for the coupling of the radiative core and the convective envelope is in the range of 20–100 Myr (Keppens et al. 1995; Allain 1998; Sills et al. 2000). The evolutionary timescale on the giant branch is comparable to and the degree of differential rotation generated by structural change on the giant branch is much greater than the differential rotation generated by main-sequence angular momentum loss.

It should be noted that the conditions needed to explain rapid horizontal-branch rotation (i.e., differential rotation on the giant branch) are the same as those required to produce mixing on the giant branch (Sweigart & Mengel 1979; Pinsonneault 1997). This is an encouraging sign for the possibility of self-consistent giant-branch mixing models.

### 4.3. *Angular Momentum Evolution on the Horizontal Branch*

In all of the classes of models that we have examined, horizontal-branch rotation rates of 1 km s$^{-1}$ or less are predicted if the giant-branch angular momentum distribution is evolved to the horizontal branch using local conservation of angular momentum. To first order, horizontal-branch rotation rates of order the main-sequence turnoff rotation rate or less are predicted. If angular momentum from the core can be redistributed to the envelope, more rapid rotation on the horizontal branch—up to 40 km s$^{-1}$—is possible for a main-sequence turnoff rotation rate of 4 km s$^{-1}$. The detection of rotation at the 40 km s$^{-1}$ level on the horizontal branch therefore requires internal angular momentum transport either during the helium flash or on the horizontal branch itself.

Hydrodynamic simulations of the helium flash generally

predict that the core can become mixed but that the whole star is not (Deupree 1996); in fact, the survival of a helium core is required to generate a horizontal-branch star rather than a helium-rich main-sequence star. The short timescale for evolution between the giant-branch tip and the horizontal branch also argues against a large-scale readjustment of the angular momentum profile prior to the actual horizontal-branch evolution. It therefore appears likely that ongoing angular momentum transport during the horizontal-branch phase will produce systematic changes in the surface rotation rate as a function of time; the sense of these changes would be that newly arrived stars on the horizontal branch would have the lowest rotation rate and the more evolved stars would have higher rotation rates. We also note that in the absence of effective angular momentum transport from core to envelope the surface rotation rates of horizontal-branch stars are predicted to be very low. These properties have interesting consequences for the interpretation of both the observed range of rotation rates at fixed effective temperature and the difference in the observed rotation rates of hotter and cooler horizontal-branch stars.

#### 4.3.1. *The Range of Horizontal-Branch Rotation Rates at Fixed $T_{\rm eff}$*

The horizontal-branch rotation data require a range in rotation velocity at fixed $T_{\rm eff}$. This is contrary to expectations from an extrapolation of trends observed on the main sequence and is larger than can be explained by a random orientation of spin axes. Indeed, Peterson et al. (1995) rejected this explanation for the range of rotation rates in M13. We believe that angular momentum evolution on the horizontal branch is responsible for this range, rather than a true range of total angular momenta at fixed horizontal-branch mass. The range of observed rotation rates at fixed mass and composition is observed to decrease strongly with increased age; e.g., compare the distribution of rotation rates in the Hyades cluster of Radick et al. (1987) with the distribution of rotation rates in the Pleiades cluster (Soderblom et al. 1993). This is a natural consequence of an angular momentum loss rate that increases with $\omega$. Different theoretical models can predict different internal angular momentum distributions in turnoff stars, but the memory of the initial conditions would be expected to be erased if either hydrodynamic mechanisms or internal gravity waves are principally responsible for internal angular momentum transport in stars. The case of internal angular momentum transport by magnetic fields (Keppens et al. 1995) is different: the overall characteristics depend on the overall internal magnetic field morphology, i.e., whether magnetic field lines connect the convective envelope with the entire radiative core. This is observationally testable: the intrinsic dispersion in rotation rates in clusters older than the Hyades can be measured directly, and a dispersion in rotation rates at older ages would be evidence of star-to-star differences in internal magnetic field morphology.

Our limiting cases, however, indicate that there is another phenomenon that must be accounted for when interpreting horizontal-branch rotation rates. The initial horizontal-branch rotation will be low for all cases. As a star evolves, internal angular momentum transport could cause the star to rotate more like a solid body, on timescales that could be comparable to the horizontal-branch lifetime of these stars. If this scenario were correct, then rotation rates of stars should increase with luminosity at approximately fixed effective temperature (i.e., along evolutionary tracks). It will be necessary to identify those stars that are evolving in $T_{\rm eff}$, on their way to the asymptotic giant branch, so as not to confuse them with those stars that have just started evolving off the zero-age horizontal branch.

#### 4.3.2. *Trends in Rotation with $T_{\rm eff}$ on the Horizontal Branch*

The models for horizontal-branch stars cooler than $\sim$12,000 K demonstrate a morphology consistent with the upper envelope of the observed rotation rates of these stars (see Fig. 7) as long as the initial angular momentum budget is high. Since the lowest temperature stars retain most of their mass, and hence their moments of inertia, they are rotating quite slowly. As temperature increases along the horizontal branch, the stars lose more mass and therefore more angular momentum, but their moments of inertia decrease more rapidly than the angular momentum loss, so the stars rotate faster as their temperature increases.

However, the abrupt drop in rotation velocity at $\sim$12,000 K and the apparent bimodal distribution of rotation rates along the horizontal branch is not predicted by our models. Since we assume that horizontal-branch temperature is solely a function of horizontal-branch mass, we predict a smooth behavior of horizontal branch properties with $T_{\rm eff}$. Any explanation that invokes different mass-loss rates on the giant branch (caused by some second parameter perhaps) must include an explanation of why a small change in mass results in a significant change in rotational properties on the horizontal branch.

There is an important additional piece of information about these hotter horizontal-branch stars: the stars hotter than 12,000 K all show evidence for gravitational settling (Behr et al. 1999). Gravitational settling of heavy elements creates mean molecular weight gradients in the outer parts of the star, which inhibits angular momentum transport in the star (Pinsonneault 1997, and references therein; Vauclair 1999). This could be an indication that, when the mean molecular weight gradients become large enough, they prevent angular momentum redistribution from the rapidly rotating core to the slowly rotating envelope. Theory predicts that this should be a threshold process wherein the mean molecular weight gradient needs to reach a critical value before the inhibition of angular momentum transport begins (Mestel 1953; Roxburgh 1991). If this explanation is correct, the rotation boundary in the horizontal branch should coincide with the gravitational settling boundary in $T_{\rm eff}$.

Giant-branch stars contain another strong gradient in the mean molecular weight, at the hydrogen-burning shell. If mean molecular weight gradients inhibit angular momentum redistribution, then the angular momentum that is interior to the hydrogen-burning shell will not be available to be redistributed throughout the star on the horizontal branch. If we assume that the horizontal-branch star rotates as a solid body outside its hydrogen-burning shell, then the rotation rate is determined by the moment of inertia of the star outside the shell and the amount of angular momentum that is available. The rotation rates in each of our four cases are given by the following formulae:

$$v(\mathrm{A}) = f_J^{\mathrm{A}} J_{\rm init} R_{\rm HB}/I_{\rm avail}^{\rm HB}\,, \tag{9}$$

$$v(\mathrm{B}) = (f_J^{\mathrm{B}} - 0.169) J_{\rm init} R_{\rm HB}/I_{\rm avail}^{\rm HB}\,, \tag{10}$$

$$v(\mathrm{C}) = f_J^{\mathrm{C}} J_{\rm init} R_{\rm HB}/I_{\rm avail}^{\rm HB}\,, \tag{11}$$

and

$$v(\mathrm{D}) = (M_{\mathrm{HB}} - M_{\mathrm{core}}) J_M^{\mathrm{D}} R_{\mathrm{HB}} / I_{\mathrm{avail}}^{\mathrm{HB}} , \quad (12)$$

where $f_J$ is the fraction of initial angular momentum retained for each case and $I_{\mathrm{avail}}^{\mathrm{HB}}$ is the moment of inertia of the star outside the hydrogen-burning shell.

For the coolest horizontal-branch stars, the majority of the star's moment of inertia is outside the shell, and the fraction drops to approximately 10% for the star with the most mass loss in Table 1. The amount of angular momentum that is outside the hydrogen-burning shell depends on the distribution of angular momentum in the star at the tip of the giant branch. The difference between the total angular momentum and the envelope angular momentum on the horizontal branch is the most important factor in this scenario. Since the moment of inertia of the envelope is quite small for the lowest mass horizontal-branch stars, the rotational velocity under the assumption of trapped core angular momentum is quite high. For the higher mass horizontal-branch stars, the rotational velocities are not significantly changed, as seen in Figure 8. Therefore, the suggestion that mean molecular weight gradients can inhibit the transport of angular momentum to the envelope is not contradicted by the presence of a hydrogen-burning shell.

### 4.4. *Other Possibilities*

We have restricted ourselves to models with solid body main-sequence rotation. As a result, the limited angular momentum budget combined with relatively rapid horizontal-branch rotation sets stringent limits on the post–main-sequence angular momentum evolution. There are some other interesting possibilities that should be mentioned.

First, there is the possibility that main-sequence stars could contain rapidly rotating cores. Even the most recent helioseismic inversions do not rule out rapid rotation in the deep solar interior, although they also provide no support for the existence of rotation rapid enough to contribute a large amount of angular momentum. If some main-sequence stars retain rapidly rotating cores, the most likely possibility is therefore that a range of internal rotation rates survives in stars to late ages; in this case the internal rotation of the Sun would simply be one of a range of possibilities. This is possible if stars have a range of overall magnetic field morphologies, with the Sun being closer to a field that strongly couples the radiative core and convective envelope and the progenitors of the rapidly rotating horizontal-branch stars presumably being stars with weak coupling. We note, however, that other mechanisms (hydrodynamic mechanisms, gravity waves) would still operate and that it is not clear that different internal rotation can survive for a Hubble time even in this case (Barnes, Charbonneau, & MacGregor 1999). This possibility would be made more likely if it can be shown that the surface rotation of the main-sequence precursors to the horizontal-branch stars have rotation rates lower than 4 km $s^{-1}$. There is a second observational test as well: if a dispersion in rotation rates at fixed mass, composition, and age is found in turnoff stars in older systems, this implies that the surface rotation rates have not converged to the high degree predicted if angular momentum transport is dominated by gravity waves or hydrodynamic mechanisms.

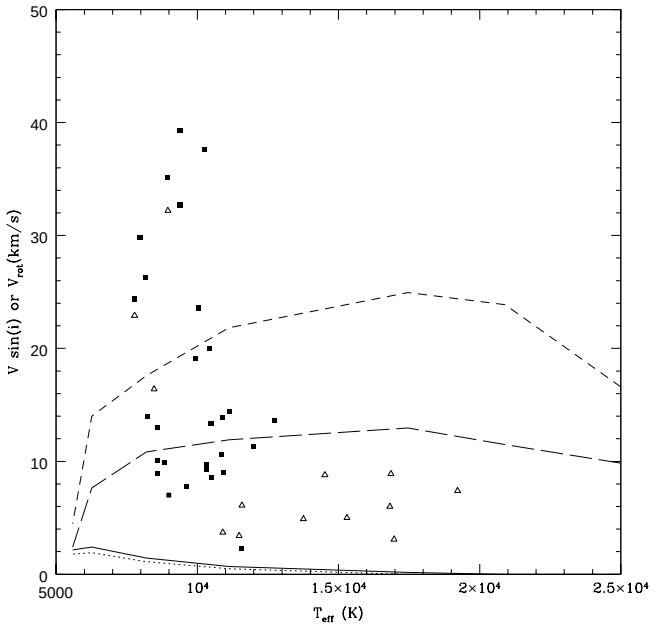


FIG. 8.—Same as Fig. 7, but using the assumption that the angular momentum and moment of inertia inside the hydrogen-burning shell is trapped and not available for determining the surface rotation rate.

Second, it is possible in a restricted set of circumstances for angular momentum to be pumped from a slowly rotating envelope into a more rapidly rotating core. The equations for meridional circulation as presented by Zahn (1991) involve the distortion from spherical symmetry both locally (a centrifugal term) and globally (a quadrupole term); furthermore, the transport of angular momentum involves both a diffusive term and an advective term. It is therefore possible, in the limit of very slow local rotation and a highly distorted core, to reverse the sign of the velocity and have a net transport of angular momentum from the envelope into the core even if the average rotation decreases with increased radius (M. H. Pinsonneault & A. Sills 2000, in preparation). This inversion requires a combination of rapid core and slow envelope rotation, and it is not clear that a main-sequence solid body rotator will develop sufficient differential rotation with depth to achieve this condition even for solid body rotation in the giant-branch convective envelope. This is, however, an interesting possibility that deserves future study. In this case angular momentum could be extracted from the envelope and deposited in the core; if the quadrupole term is sufficiently large, it could even drive large-scale mixing in the envelope of the giant-branch star in the presence of slow local rotation.

Third, we cannot rule out the possibility of a source of angular momentum on the giant branch itself. A nonaxisymmetric helium flash is one possibility; another would be mass transfer between close binaries or between single stars and nearby giant planets (Soker 1998). The first case could potentially be tested by comparing the velocity dispersion of horizontal-branch stars relative to giants, since we would expect that a nonaxisymmetric helium flash should impart linear as well as angular momentum to the horizontal-branch star. For the second case, mass and angular momentum transfer from a companion is certainly possible; a merger of two stars either through collisions or binary mergers is thought to be the origin of the blue strag-

gler phenomenon (Bailyn 1995). However, one important problem with these explanations is that the frequency of nearby brown dwarfs and giant planets appears to be small, of order 5% (Marcy et al. 1998), while the binary fraction in globular clusters is about 20% (Hut et al. 1992). Cluster-to-cluster differences in horizontal-branch rotation rates and the observed trends with $T_{\rm eff}$ on the horizontal branch would also have to be accounted for.

A possible explanation of the bimodal distribution in rotation rates with $T_{\rm eff}$ is the existence of two separate populations of stars on the horizontal branch. The correlation between the sharp cutoff in rotation rates and the existence of a gap in the horizontal branch of M13 has prompted speculation that two populations are present in this cluster, but the reason for these two populations is not yet apparent. Dynamically created populations, such as evolved blue stragglers or giant-branch stars stripped by close encounters with other stars, are candidates for this class of explanation. It is difficult to understand, however, how the small populations of blue stragglers or stars with binary systems could evolve to become as numerous on the horizontal branch as the normal horizontal-branch stars in the cluster.

The work presented here is an initial study of some physically interesting limiting cases. The simplified prescription of giant-branch evolution presented in this paper neglects some physical effects that can change the structure and angular momentum profile of the horizontal-branch stars. Rotation also affects the structure of the star, both directly and indirectly. Since rotation can provide an additional source of support for the star, the core temperature of the star will be lower than that of a nonrotating star. Therefore, the star can live on the giant for longer until the core temperature becomes high enough for the helium flash to occur. This will result in a larger core mass than a nonrotating star, and will also increase the amount of mass loss that can occur on the giant branch (Mengel & Gross 1976). The internal transport of angular momentum during giant-branch evolution will be more complicated than the simple prescriptions presented in this paper and could also modify giant-branch evolution enough to change the position of the star in the H-R diagram, the core mass at helium flash, and the amount of mass loss. We are planning to follow giant-branch evolution, include the effects of rotation, using machinery already present in the code, and consider advection and angular momentum transport by gravity waves.

## 5. SUMMARY

Stellar rotation is an important phenomenon, and there is a large and growing body of data that is most easily interpreted as evidence for rotationally induced mixing in stars. The principal difficulty in including rotation in theoretical stellar evolution calculations has been the uncertainty about the internal angular momentum distribution of stars. We believe that the horizontal-branch rotation data shed some new and interesting light on this problem. Evolved stars provide complementary information to the extensive studies of rotation in the Sun and low-mass main-sequence stars.

We have calculated simple models of angular momentum evolution on the giant branch, concentrating on several limiting cases for the internal angular momentum profiles on the giant branch and horizontal branch. We find that rapid rotation on the horizontal branch can be reconciled with solid body main-sequence rotation if giant-branch stars have differential rotation in their convective envelopes and rapidly rotating cores, which is then followed by a redistribution of angular momentum on the horizontal branch. This set of conditions are the same as the conditions that most favor mixing on the giant branch. A rotation rate of $\sim 4$ km s$^{-1}$ at the main-sequence turnoff is required to explain the high rotation rates for the cooler horizontal-branch stars.

We suggest that the observed range in rotation rates for the cool horizontal-branch stars is a consequence of angular momentum evolution on the horizontal branch. Angular momentum could be transported from the core to the envelope over the horizontal-branch lifetime of the star, producing a correlation between rotation rate and luminosity on the horizontal branch. Our models do not predict the sharp cutoff in rotation rates seen in the hot horizontal-branch stars in M 13. We suggest that this discontinuity is not tied to the angular momentum loss rate from the giant branch but rather could be a result of gravitational settling. This creates a mean molecular weight gradient in the star, which then inhibits angular momentum transport in the star.

We have proposed two observational tests pertaining to main-sequence stars that would be very useful in providing clarity to the problem of angular momentum evolution on the giant branch. We need to know the surface rotation rates of Population II main-sequence stars to constrain the total angular momentum budget that is available for loss and redistribution on the giant and horizontal branches. Also, by studying the dispersion, or lack thereof, in rotational velocities of main-sequence stars in old open clusters, we can determine how the internal magnetic field morphology could affect the dispersion in total angular momenta in main-sequence stars.

It would clarify the problem considerably to gather more observational data on rotation rates of horizontal-branch stars in globular clusters. First, is the sharp cutoff in rotation rates seen in M 13 statistically significant? The data presented so far are convincing, but only seven of the approximately 25 stars hotter than 13,000 K have been observed. Better statistics would eliminate this uncertainty. It would also be of great interest to observe the same kinds of stars in other globular clusters. We already know that horizontal-branch morphology varies from one cluster to another. If we can determine that this cutoff in rotation rates is ubiquitous or, alternatively, that it is correlated with horizontal-branch morphology, that will provide a valuable clue in determining the cause of the second parameter effect and in understanding angular momentum evolution on the giant branch. Second, we suggest that observers search for correlations between rotation rates and surface abundances in horizontal-branch stars to determine if there is a clear relationship between gravitational settling and rotational properties on the horizontal branch.

This work was supported by NASA grant NAG5-7150. A. S. wishes to recognize support from the Natural Sciences and Engineering Research Council of Canada. The authors would like to thank the referee for a careful and thorough reading of the manuscript.

REFERENCES

Alexander, D. R., & Ferguson, J. W. 1994, ApJ, 437, 879
Allain, S. 1998, A&A, 333, 629
Allard, F., & Hauschildt, P. H. 1995, ApJ, 445, 433
Bailyn, C. D. 1995, ARA&A, 33, 133
Barnes, G., Charbonneau, P., & MacGregor, K. P. 1999, ApJ, 511, 466
Behr, B. B., Cohen, J. G., McCarthy, J. K., & Djorgovski, S. G. 1999, ApJ, 517, L135
Behr, B. B., Djorgovski, S. G., Cohen, J. G., McCarthy, J. K., Côté, P., Piotto, G., & Zoccali, M. 2000, ApJ, 528, 849
Boothroyd, A. I., & Sackmann, I.-J. 1999, ApJ, 510, 232
Carney, B. W., & Peterson, R. C. 1981, ApJ, 251, 190
Chaplin, W. J., et al. 1999, MNRAS, 308, 405
Charbonnel, C. 1995, ApJ, 453, L41
Cohen, J. G., & McCarthy, J. K. 1997, AJ, 113, 1353
Corbard, T., Di Mauro, M. P., Sekii, T., & the GOLF Team. 1998, in Proc. SOHO6/GONG98 Workshop, Structure and Dynamics of the Interior of the Sun and Sun-like Stars, ed. S. Korzennik & A. Wilson (ESA SP-418; ESA: Noordwijk), 741
Deupree, R. G. 1996, ApJ, 471, 377
Durney, B. R., & Latour, J. 1978, Geophys. Astrophys. Fluid Dyn., 9, 241
Gould, A. 1997, ApJ, 483, 98
Hobbs, L. M., Thorburn, J. A., & Rebull, L. M. 1999, ApJ, 523, 797
Hut, P., et al. 1992, PASP, 104, 981
Iglesias, C. A., & Rogers, F. J. 1996, ApJ, 464, 943
Keppens, R., MacGregor, K. B., & Charbonneau, P. 1995, A&A, 294, 469
Kraft, R. 1965, ApJ, 142, 681
Lazrek, M., et al. 1996, Sol. Phys., 166, 1
Lee, Y.-W., Demarque, P., & Zinn, R. 1990, ApJ, 350, 155
Marcy, G. W., Butler, P., Vogt, S., & Shirts, P. 1998, BAAS, 192, 801
Mengel, J. G., & Gross, P. G. 1976, Ap&SS, 41, 407
Mestel, L. 1953, MNRAS, 113, 716
Michaud, G., & Charbonneau, P. 1991, Space Sci. Rev., 57, 1
Peterson, R. C. 1983, ApJ, 275, 737
———. 1985a, ApJ, 289, 320
———. 1985b, ApJ, 294, L35
Peterson, R. C., Tarbell, T. D., & Carney, B. W. 1983, ApJ, 265, 972
Peterson, R. C., Rood, R. T., & Crocker, D. A. 1995, ApJ, 453, 214
Pinsonneault, M. H. 1997, ARA&A, 35, 557
Pinsonneault, M. H., Deliyannis, C. P., & Demarque, P. 1991, ApJ, 367, 239
Radick, R. R., Thompson, D. T., Lockwood, G. W., Duncan, D. K., & Baggett, W. E. 1987, ApJ, 321, 459
Reimers, D. 1991, in Problems in Stellar Atmospheres and Envelopes, ed. B. Baschek, W. H. Kagel, & G. Traving (New York: Springer)
Rogers, F. J., Swenson, F. J., & Iglesias, C. A. 1996, ApJ, 456, 902
Rood, R. T. 1973, ApJ, 184, 815
Roxburgh, I. 1991, in Angular Momentum Evolution of Young Stars, ed. S. Catalano & J. Stauffer (Dordrecht: Kluwer)
Saumon, D., Chabrier, G., & Van Horn, H. M. 1995, ApJS, 99, 713
Sills, A., Pinsonneault, M. H., & Terndrup, D. M. 2000, ApJ, 534, 335
Soderblom, D. R., Stauffer, J. R., MacGregor, K. B., & Jones, B. F. 1993, ApJ, 409, 624
Soker, N. 1998, AJ, 116, 1308
Sweigart, A. 1997, ApJ, 474, L23
Sweigart, A. V., & Mengel, J. G. 1979, ApJ, 229, 624
Talon, S., Zahn, J.-P., Maeder, A., & Meynet, G. 1997, A&A, 322, 209
Thompson, M. J., et al. 1996, Science, 272, 1300
Vauclair, S. 1999, A&A, 351, 973
Zahn, J.-P. 1991, A&A, 252, 179